

Incorporation of Copper in SiBEA Zeolite as Isolated Lattice Mononuclear Cu(II) Species and its Role in Selective Catalytic Reduction of NO by Ethanol

Stanislaw Dzwigaj · Janusz Janas · Jan Mizera ·
Jacek Gurgul · Robert P. Socha · Michel Che

Received: 17 July 2008 / Accepted: 15 September 2008 / Published online: 2 October 2008
© Springer Science+Business Media, LLC 2008

Abstract The Cu_xSiBEA zeolites prepared by a two-step postsynthesis method are active in selective catalytic reduction of NO by ethanol and their catalytic activity is related to the presence of mononuclear Cu(II) species. Zeolite with isolated lattice mononuclear Cu(II) species is active in this reaction with selectivity toward dinitrogen close to 70–90%.

Keywords SiBEA zeolite · Copper · NO · Ethanol · XRD · DR UV–vis · XPS · TPR

1 Introduction

Removal of NO_x is one of the most significant environmental problems, particularly because of the associated destruction of the ozone layer. Since the discovery in 1986 by Iwamoto et al. of the remarkable activity of Cu-ZSM-5 catalysts in NO decomposition [1] and then in the selective catalytic reduction (SCR) of NO with hydrocarbons [2],

much work has been performed to understand the role of copper in comparison to other transition metal ions exchanged in zeolite [1–4]. It has been reported [5] that the most active sites for SCR of NO and NO decomposition in Cu-ZSM-5 involve Cu(II) and Cu(I), respectively, both adjacent to framework Al atoms. This would suggest that for both processes, the presence of Al in the environment of Cu ions is necessary in the formation of active sites, as it has been recently stated [6].

The present contribution reports on the preparation of Cu-containing dealuminated BEA zeolite by a two-step postsynthesis method. This method allows to introduce copper as isolated mononuclear Cu(II) species and to obtain CuSiBEA catalysts with no Al in the Cu environment. Our results indicate that the SCR of NO by ethanol may occur on isolated lattice mononuclear Cu(II) species after Al atoms have been removed from the zeolite structure.

In the present work, the speciation of copper and relationship between structure of Cu species and its properties in the selective catalytic reduction of NO by ethanol in Cu_xSiBEA zeolites is investigated.

2 Experimental Section

2.1 Materials

Cu_xSiBEA zeolites are prepared by the two-step postsynthesis method reported earlier [7, 8] which consists of first creating vacant T-sites with associated silanol groups by dealumination of TEABEA zeolite with nitric acid and then impregnating the resulting SiBEA zeolite with an aqueous solution of $\text{Cu}(\text{NO}_3)_2$. To obtain well dispersed copper species, Cu_xSiBEA zeolites are prepared with low Cu content

S. Dzwigaj · M. Che
Laboratoire de Réactivité de Surface, UPMC Univ Paris 6,
UMR 7609, 4 Place Jussieu, 75252 Paris Cedex 05, France

S. Dzwigaj (✉) · M. Che
Laboratoire de Réactivité de Surface, CNRS, UMR 7609,
4 Place Jussieu, 75252 Paris Cedex 05, France
e-mail: stanislaw.dzwigaj@upmc.fr; dzwigaj@ccr.jussieu.fr

J. Janas · J. Mizera · J. Gurgul · R. P. Socha
Institute of Catalysis and Surface Chemistry, Polish Academy
of Sciences, ul. Niezapominajek 8, 30-239 Krakow, Poland

M. Che
Institut Universitaire de France, 103 Boulevard Sain-Michel,
75005 Paris, France

(1.4 and 1.8 Cu wt%). For this, 2 g of SiBEA zeolite (Si/Al > 1,300), obtained by treatment of a tetraethyl ammonium BEA zeolite (Si/Al = 11) (provided by RIPP-China) in an aqueous 13 mol L⁻¹ HNO₃ solution (4 h, 353 K), is stirred for 24 h at 298 K in aqueous solutions containing 6.3×10^{-3} and 9×10^{-3} mol L⁻¹ of Cu(NO₃)₂·3H₂O. Then, the suspension is stirred for 2 h in air at 353 K until the water is completely evaporated. The solid is washed and then dried in air at 353 K for 24 h. The resulting Cu_{1.4}SiBEA and Cu_{1.8}SiBEA samples are pale blue.

2.2 Techniques

Powder X-ray diffractograms (XRD) are recorded on a Siemens D5000 using the CuK_α radiation ($\lambda = 154.05$ pm).

Diffuse reflectance UV–vis (DR UV–vis) spectra are recorded on a Cary 5E spectrometer equipped with an integrator and a double monochromator.

XPS experiments are performed in ultra high vacuum (UHV) system at a pressure of approximately of 10⁻⁷ Pa. The system is equipped with hemispherical analyzer SES R4000 (Gammatdata Scienta) and AlK_α (1486.6 eV) X-ray source. The power of the X-ray source is 240 W and the analyzer pass energy is set as 100 eV, which corresponds to FWHM of 0.9 eV for the Ag 3d_{5/2} excitation. The work function of the spectrometer is calibrated according to ISO 15472:2001 procedure using Cu, Au and Ag foils as references. The electron binding energies (BE) for Si, O and Cu are measured by taking the C1s peak at 285.0 eV as the internal standard.

XPS data are obtained on fresh (Cu_xSiBEA calcined in flowing air for 3 h at 773 K) or used catalysts (Cu_xSiBEA after catalytic test, sample calcined in dry air at 453 K). Prior to XPS analysis, the samples are evacuated to 10⁻⁷ Pa. The background in all spectra is approximated by the Shirley type function. The spectra are deconvoluted into components by applying Voigt profile (70:30 mixture of Gaussian/Lorentzian shape).

Temperature-programmed reduction (TPR) experiments are performed on Quanatachrome Chembet 3000 apparatus, TPR/TPD Option. The reduction of 0.1 g zeolite sample is carried out from 320 to 1,120 K in a flow of 5% H₂ in Ar at 10 K min⁻¹. The H₂ consumption is monitored by a thermal conductivity detector (TCD). Prior to reduction, the samples are pre-treated at 453 K in He (in the case of used samples) or at 733 K in flowing O₂/He mixture for 3 h (in the case of fresh samples).

2.3 Catalysis Measurements

The activity of catalysts in the SCR of NO with ethanol or propane is measured in a conventional flow reactor coupled

to a gas chromatograph. The composition of the feed is: 1,000 ppm NO, 1,000 ppm ethanol, the mixture of 2 vol.% O₂ in He with a catalyst volume of 1 mL and a 10,000 h⁻¹ gas hour space velocity. Before catalytic tests, the sample is heated up to 523 K in oxygen/helium mixture and then NO and ethanol vapour streams are switched on. The standard conditions are: 2 h catalytic runs at 523–623 K and 1 h runs at higher reaction temperature (NO_x and CO_x concentrations at the reactor outlet are continuously monitored to check if pseudo steady-state conditions are established). The reaction temperature is increased every 50 K interval up to 773 K and then lowered in the same way to 523 K. In the case of NO conversion or product selectivity measurements, the heating sequence is repeated to obtain real steady-state reaction conditions in the whole reaction temperature range. Only for NO oxidation experiments in absence of ethanol, heating of the catalysts in the mixture containing 2 vol.% O₂ in He over 723 K for 1 h is necessary in order to obtain a reproducible activity.

All conversion and selectivity values used in the text are defined and calculated in standard manner and presented in mol.%. Because of difficulties with the straight determination of N₂ concentration at the reactor outlet, the selectivity to dinitrogen is determined as follows:

$$S_{N_2} = 100 - (S_{NO_2} + S_{N_2O} + S_{NH_3} + S_{OrgN}),$$

where S_{NO₂}, S_{N₂O} and S_{NH₃} are the selectivity into NO₂, N₂O and ammonia, respectively and S_{OrgN} is the sum of selectivities into nitrogen-containing organic compounds.

3 Results and Discussion

3.1 Incorporation of Copper into the Framework of Dealuminated BEA

3.1.1 X-ray Diffraction and FTIR Spectroscopy

XRD patterns of AIBEA, SiBEA, Cu_{1.4}SiBEA and Cu_{1.8}SiBEA typical of BEA zeolite are very similar (Fig. 1). It shown that the crystallinity of BEA zeolite is preserved after dealumination and then incorporation of copper ions. All the samples do not show any evidence of extra lattice crystalline compounds or long-range amorphization of the zeolite. A change of the position of the narrow main diffraction peak around 2θ of 22.60° generally taken as evidence of lattice contraction/expansion of the BEA structure [9, 10], from 22.55 to 22.71° after dealumination indicates contraction of the matrix. The d₃₀₂ spacing obtained from this peak decreases from 3.942 (AIBEA) to 3.912 Å (SiBEA).

In contrast, the decrease of the 2θ value after introduction of Cu ions indicates expansion of the BEA structure and suggests that the latter are incorporated into the lattice.

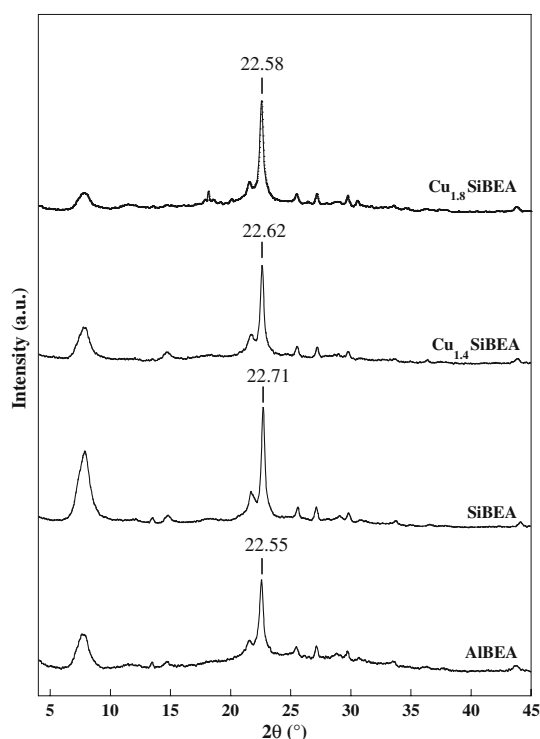


Fig. 1 X-ray diffractograms recorded at room temperature of AlBEA, SiBEA, $\text{Cu}_{1.4}\text{SiBEA}$ and $\text{Cu}_{1.8}\text{SiBEA}$

The d_{302} spacing related to the peak near 22.60° increases from 3.912 (SiBEA) to 3.940 Å ($\text{Cu}_{1.4}\text{SiBEA}$) (with 2θ of 22.62°) and to 3.941 Å ($\text{Cu}_{1.8}\text{SiBEA}$) (with 2θ of 22.58°) (Fig. 1).

The treatment of AlBEA zeolite with aqueous HNO_3 solution involves the elimination of Al atoms from the framework, as evidenced by the disappearance of IR bands at 3,781, 3,665 and $3,609\text{ cm}^{-1}$ attributed to AlO-H and Si-O(H)-Al groups, respectively (results not shown), in line with earlier investigations [7, 8]. The appearance of narrow bands at 3,736 and $3,710\text{ cm}^{-1}$ related to isolated internal silanol groups and of a broad band at $3,520\text{ cm}^{-1}$ due to H-bonded SiOH groups in SiBEA reveals the presence of vacant T-sites associated with silanol groups, as shown earlier [11]. The incorporation of copper leading to Cu_xSiBEA induces a reduction of intensity of these bands, suggesting that silanol groups are consumed in the reaction with copper precursor.

3.2 Dependence of Copper Speciation on the Copper Content in Cu_xSiBEA

3.2.1 Diffuse Reflectance UV-vis Spectroscopy

Figure 2 shows the DR UV-vis spectra of as prepared $\text{Cu}_{1.4}\text{SiBEA}$ and $\text{Cu}_{1.8}\text{SiBEA}$. The spectrum of $\text{Cu}_{1.4}\text{SiBEA}$ is composed only of a broad band at around 780 nm

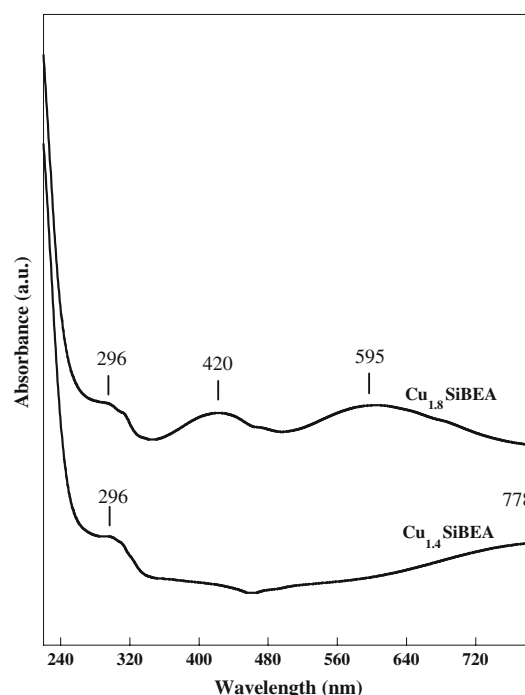


Fig. 2 UV-vis spectra recorded at room temperature of as prepared $\text{Cu}_{1.4}\text{SiBEA}$ and $\text{Cu}_{1.8}\text{SiBEA}$

attributed to d-d transition of Cu^{2+} ($3d^9$) ions and another one at 296 nm attributed to charge transfer (CT) $\text{O}^{2-} \rightarrow \text{Cu}^{2+}$ transitions between lattice oxygen and Cu^{2+} ion [12–15]. In contrast, in the spectrum of $\text{Cu}_{1.8}\text{SiBEA}$ apart of the charge transfer (CT) $\text{O}^{2-} \rightarrow \text{Cu}^{2+}$ transitions (296 nm), the broad bands at 420 and 595 nm are observed assigned to CT $\text{O}^{2-} \rightarrow \text{Cu}^{2+}$ and d-d transitions of extra-lattice octahedral Cu(II) species, respectively, in line with earlier reports [16, 17]. These results show that in $\text{Cu}_{1.4}\text{SiBEA}$ mainly isolated mononuclear Cu(II) species are present. However, in $\text{Cu}_{1.8}\text{SiBEA}$ besides of mononuclear Cu(II) species also extra-lattice octahedral Cu(II) species (polynuclear copper-oxygen complexes or probably minor amounts of copper oxide) appear.

3.2.2 X-ray Photoelectron Spectroscopy

The Si 2p, O 1s and Cu 2p core level excitation are analyzed for all of the zeolite samples whereas only Cu 2p spectra are shown in Figs. 3 and 4. The spectra are deconvoluted into minimal number of peaks taking into account the measurement resolution ($<0.9\text{ eV}$), type of excitation and chemical composition of the samples investigated. The peak parameters are collected in Table 1. Since Cu $2p_{3/2}$ excitation alone does not allow determine without doubt the oxidation state and coordination of copper, Cu-containing zeolites have been characterized by using X-ray excited Cu $2p_{3/2}$ and Cu L_3VV transitions, the

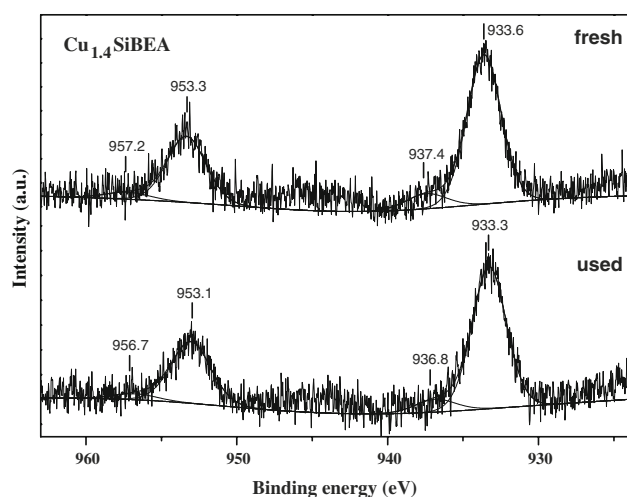


Fig. 3 XPS spectra recorded at room temperature of Cu 2p core level of fresh and used $\text{Cu}_{1.4}\text{SiBEA}$

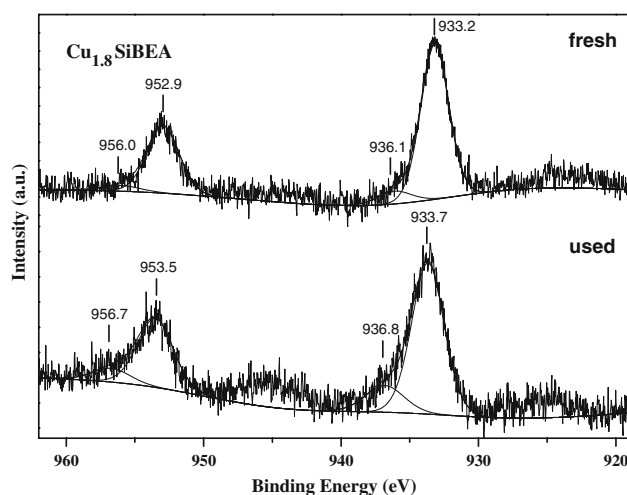


Fig. 4 XPS spectra recorded at room temperature of Cu 2p core level of fresh and used $\text{Cu}_{1.8}\text{SiBEA}$

modified Auger parameter and the shake-up satellite associated to Cu $2p_{3/2}$ peak. In most cases, Cu(II) species show a shake-up satellite at electron binding energy of ca. 10 eV higher than the Cu $2p_{3/2}$ transition, which is not observed for Cu(I) and Cu(0) species. This feature can be

used to distinguish between Cu(II) and Cu(I) or Cu(0). As was shown for ZSM-5 doped with Cu [18], the kinetic energy of Auger excitation related to Auger parameter provides an efficient tool to describe location and aggregation of Cu ions.

As shown in Figs. 3 and 4, Cu 2p spectra obtained for both $\text{Cu}_{1.4}\text{SiBEA}$ and $\text{Cu}_{1.8}\text{SiBEA}$ (fresh and used) are deconvoluted into two doublets. For all samples, the most intensive peak of Cu $2p_{3/2}$ excitation shows the binding energy slightly larger than 933 eV and the second peak with energy above 936 eV. Taking into account the value of binding energy, both peaks can be assigned to Cu(II), in line with earlier reports [18, 19]. The other feature characteristic for Cu(II) species incorporated in BEA zeolite (Table 1) is low kinetic energy of Cu L_3VV Auger excitation (between 913.0 and 913.5 eV), not shown in Figs. 3 and 4, that suggests the presence of Cu(II) species inside of zeolite structure.

The SCR of NO performed on $\text{Cu}_{1.8}\text{SiBEA}$ results in a shift of electron binding energy of all Cu 2p peaks of 0.5–0.7 eV. Additionally, the ratio of the intensity of Cu $2p_{3/2}$ peaks with bending energy close to 933 and 936 eV decreases from about 10.0 to 4.8 and the shake-up satellites grow up. Moreover, a small decrease of the Cu/Si ratio is also observed for $\text{Cu}_{1.8}\text{SiBEA}$ after SCR reaction.

$\text{Cu}_{1.4}\text{SiBEA}$, with lower Cu content, shows little different features of XPS spectrum after SCR of NO reaction in comparison with $\text{Cu}_{1.8}\text{SiBEA}$. After SCR of NO reaction, Cu 2p binding energies for all peaks are shifted to the lower values of about 0.2–0.6 eV. The intensity of shake-up satellite remains unchanged whereas the ratio of the intensity of Cu $2p_{3/2}$ peaks at about 933 and 936 eV increases from about 8.3 to 9.4 simultaneously with increases of Cu L_3VV kinetic energy of about 0.3 eV. For this sample, the Cu/Si ratio slightly increases after SCR reaction.

The XPS results indicate that a little changes of environment of copper take place in the Cu_xSiBEA catalyst upon SCR of NO. It shows relatively strong interaction between Cu(II) and framework oxygen confirming that copper has been incorporated into vacant T-sites of SiBEA zeolite and is mainly present as isolated lattice mononuclear Cu(II) species.

Table 1 XPS data for $\text{Cu}_{1.8}\text{SiBEA}$ and $\text{Cu}_{1.4}\text{SiBEA}$ zeolites

Peak	Fresh $\text{Cu}_{1.8}\text{SiBEA}$	Used $\text{Cu}_{1.8}\text{SiBEA}$	Fresh $\text{Cu}_{1.4}\text{SiBEA}$	Used $\text{Cu}_{1.4}\text{SiBEA}$
Cu $2p_{3/2}$	933.2	933.7	933.6	933.3
Cu $2p_{3/2}$	936.1	936.8	937.4	936.8
Cu $2p_{1/2}$	952.9	953.5	953.3	953.1
Cu $2p_{1/2}$	956.0	956.7	957.2	956.7
Cu L_3VV (KE)	913.5	913.5	913.0	913.3

The table shows values of electron binding energy, except the Cu L_3VV excitation where kinetic energy (KE) is considered

3.2.3 Temperature Programmed Reduction

The TPR profiles of both $\text{Cu}_{1.4}\text{SiBEA}$ and $\text{Cu}_{1.8}\text{SiBEA}$ zeolites, treated in flowing O_2/He at 773 K, are very similar. They reveal two main TPR peaks at about 500–550 and 620–770 K due to the reduction of $\text{Cu(II)}\text{--Cu(I)}$ and $\text{Cu(I)}\text{--Cu(0)}$, respectively, in line with earlier observations by TPR on Cu-containing zeolites [12, 20–23]. The first TPR peak observed at relatively low temperature indicates a high reducibility of Cu(II) for both $\text{Cu}_{1.4}\text{SiBEA}$ and $\text{Cu}_{1.8}\text{SiBEA}$. Two peaks at 620–770 K temperature range indicate the presence of copper in two different states.

After SCR reaction and subsequent treatment at 453 K in flowing He, the TPR profiles of both samples changes in characteristic manner, leaving the first, low-temperature TPR peak at about 515–530 K practically unchanged but significant changes appear in positions and intensities of the peaks at 620–770 K temperature range. It suggests that upon SCR reaction the changes of environment of copper takes place (Figs. 5, 6).

3.3 Catalytic Activity of Cu_xSiBEA Zeolite in the SCR of NO

Figures 7 and 8 compare the activity of dealuminated SiBEA and two Cu containing SiBEA zeolites in SCR of NO by ethanol. Dealuminated SiBEA shows very low activity and NO conversion which does not exceed 7% in the whole temperature range (520–775 K). The high ethanol conversion reaching 90% at 623 K is mainly due to dehydration of ethanol but not to alcohol oxidation. The maximum yield of N_2 for SiBEA reaches only 5% at 675 K (Fig. 9).

As shown in Figs. 7 and 8, the incorporation of Cu in the SiBEA leads to obtain a more active catalyst. Indeed, for

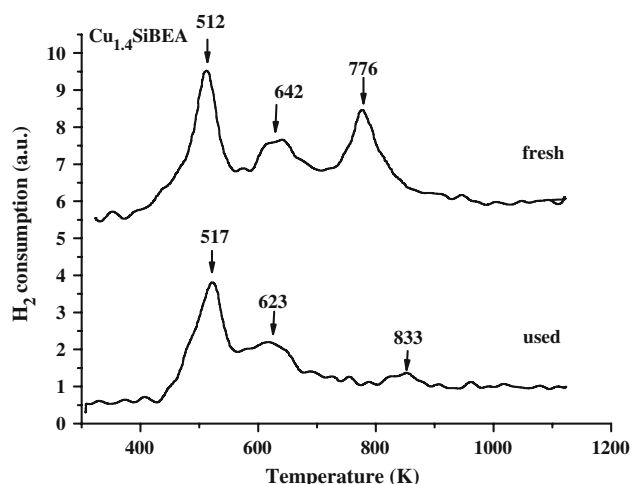


Fig. 5 TPR patterns recorded at room temperature of fresh and used $\text{Cu}_{1.4}\text{SiBEA}$

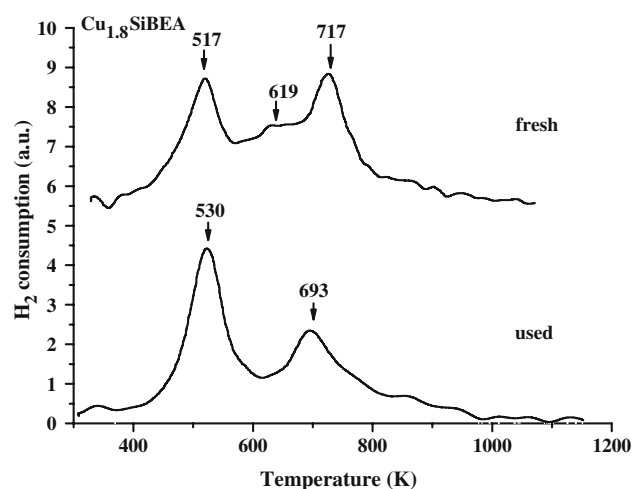


Fig. 6 TPR patterns recorded at room temperature of fresh and used $\text{Cu}_{1.8}\text{SiBEA}$

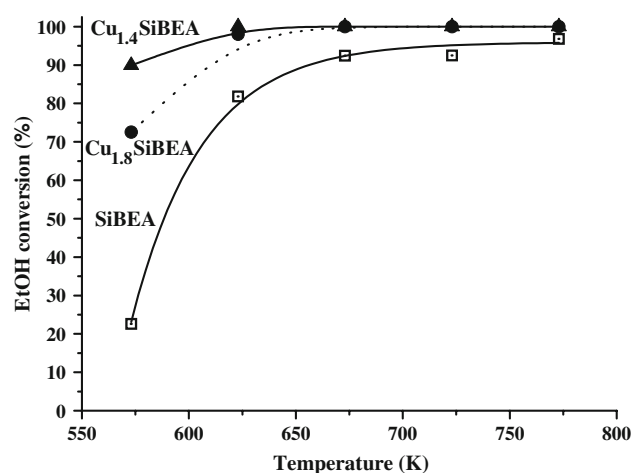


Fig. 7 Temperature-dependence of ethanol conversion in SCR of NO by ethanol on SiBEA, $\text{Cu}_{0.8}\text{SiBEA}$ and $\text{Cu}_{1.8}\text{SiBEA}$

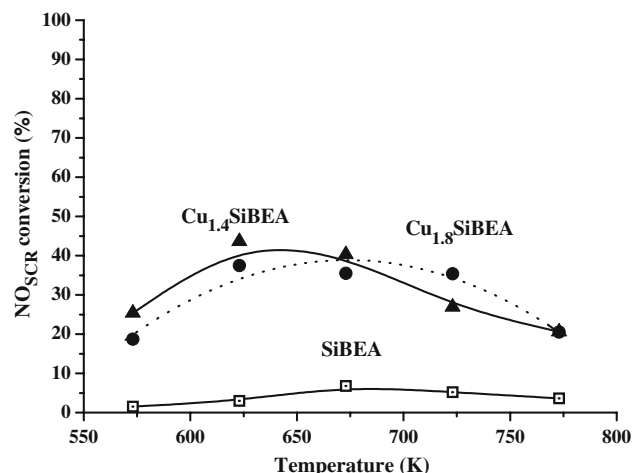


Fig. 8 Temperature-dependence of NO conversion in SCR of NO by ethanol on SiBEA, $\text{Cu}_{0.8}\text{SiBEA}$ and $\text{Cu}_{1.8}\text{SiBEA}$

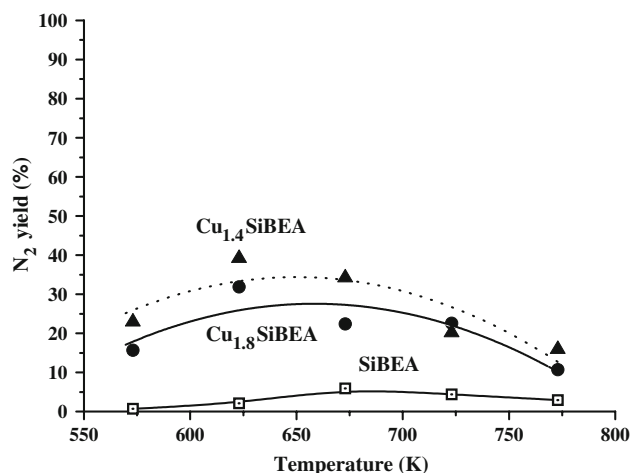


Fig. 9 Temperature-dependence of N_2 yield in SCR of NO by ethanol on SiBEA, $Cu_{0.8}SiBEA$ and $Cu_{1.8}SiBEA$

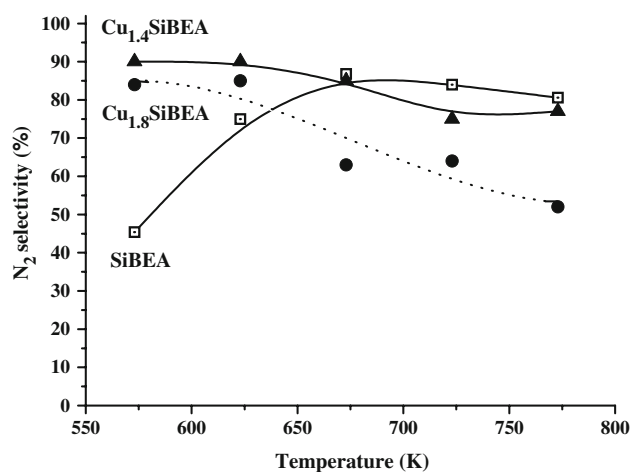


Fig. 10 Temperature-dependence of N_2 selectivity in SCR of NO by ethanol on $Cu_{0.8}SiBEA$ and $Cu_{1.8}SiBEA$

$Cu_{1.4}SiBEA$ and $Cu_{1.8}SiBEA$, a substantial increase of the SCR of NO activity is observed with a maximum NO conversion of 45% ($Cu_{1.4}SiBEA$) and 35% ($Cu_{1.8}SiBEA$) (Fig. 8) and yield of N_2 reaches 35 and 25% (Fig. 9). These results confirm that the presence of copper ions in the zeolite structure is necessary to promote the activity in the SCR of NO. Moreover, the selectivity strongly depends on the form of copper present in the dealuminated zeolite. It is much more higher for $Cu_{1.4}SiBEA$ with mainly isolated lattice mononuclear Cu(II) species (78–90%) than for $Cu_{1.8}SiBEA$ with the mixture of lattice mononuclear and extra-lattice polynuclear Cu(II) species (55–85%) in the whole temperature range (Fig. 10).

When the ethanol conversion reaches 100% with low amounts of mild oxidation products (CO and other organic products), NO_2 appears and its amount increases from 650 to 775 K (Fig. 11). The conversion of NO into NO_2 is much higher for $Cu_{1.8}SiBEA$ (maximum of about 50% at

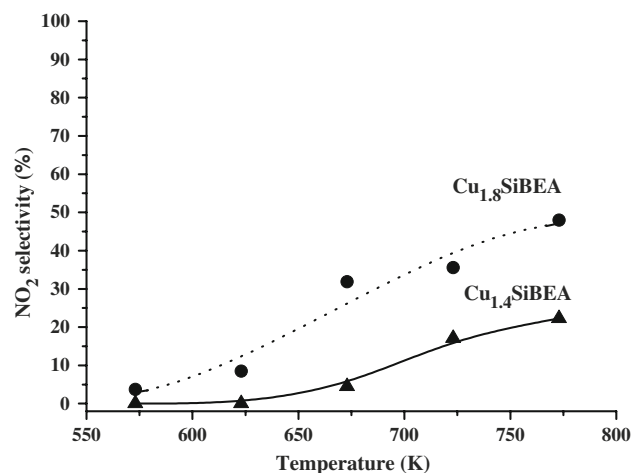


Fig. 11 Temperature-dependence of NO_2 selectivity in SCR of NO by ethanol on $Cu_{0.8}SiBEA$ and $Cu_{1.8}SiBEA$

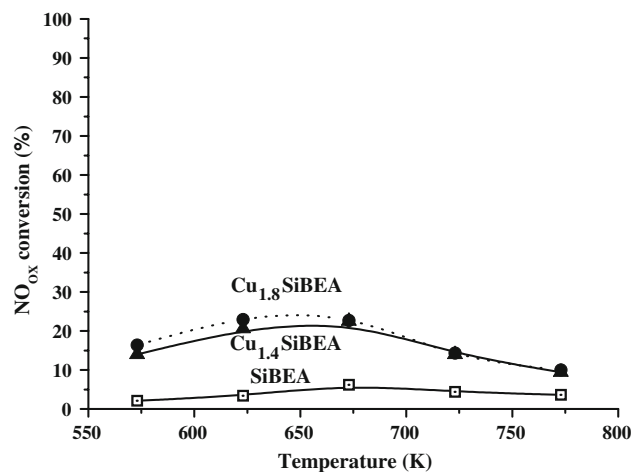


Fig. 12 Temperature-dependence of NO conversion in the absence of ethanol on SiBEA, $Cu_{0.8}SiBEA$ and $Cu_{1.8}SiBEA$

775 K) than for $Cu_{1.4}SiBEA$ (maximum of about 25% at 775 K) (Fig. 11).

The temperature dependence of NO conversion by ethanol as reducing agent (Fig. 8) shows a volcano-shape behavior, typical of various catalytic systems (Cu-exchanged natural zeolite [24], Co-exchanged MFI [25], CoSiBEA [26] and FeSiBEA [27]) and reveals the transition from a kinetic regime (presence of organic molecules in the reaction zone) to a thermodynamic one (NO/NO_2 equilibrium, when organic molecules are exhausted).

The experiments performed on $Cu_{1.4}SiBEA$ and $Cu_{1.8}SiBEA$ reveal that the conversion of NO in oxidation reaction (in absence of ethanol) is much lower than that in the SCR of NO by ethanol (Fig. 12). It suggests that copper species present in both zeolites are active sites of the latter process. However, it is important to point out that the catalytic activity of $Cu_{1.8}SiBEA$ in the SCR of NO by ethanol is a lower than that of $Cu_{1.4}SiBEA$. The difference

is probably due to the presence in $\text{Cu}_{1.8}\text{SiBEA}$ more amounts of extra-lattice polynuclear Cu(II) species that favor the oxidation of NO toward NO_2 , in particular at high temperature (Fig. 11).

We suggest that the first reaction step in SCR of NO on Cu_xSiBEA consists of the activated adsorption of NO on isolated mononuclear Cu(II) species. In the second step, the oxidation of nitrosonium by adsorbed oxygen resulting in an NO_2 adsorbed complex. The rate determining step (rds) of the SCR process could be the activated adsorption of the organic molecule followed by the surface reaction. Then in the two competitive reaction steps, either N_2 and/or NO_2 could be formed depending on the reaction temperature. Thus, the desorption of the adsorbed NO_x species to the gas phase as NO_2 seems not to be a necessary step of the SCR process on CuSiBEA catalyst.

4 Conclusions

The combined use of XRD, DR UV–vis, FTIR, XPS and TPR gives evidence that copper incorporated in SiBEA zeolite by the two-step postsynthesis method is present mainly as isolated lattice mononuclear Cu(II) species. The incorporation of Cu into the vacant T-sites of SiBEA is evidenced by XRD, while consumption of OH groups of Cu_xSiBEA is monitored by FTIR. The presence of Cu in the (II) oxidation state and mainly as mononuclear Cu(II) species is evidenced by combined use of DR UV–vis, XPS and TPR.

Zeolite $\text{Cu}_{1.4}\text{SiBEA}$ with mainly isolated lattice mononuclear Cu(II) species is active in SCR of NO by ethanol with selectivity toward N_2 close to 90–78% at the 575–778 K temperature range and maximum NO conversion of 45% at 625 K. These results indicate that the SCR of NO by ethanol may occur on isolated mononuclear Cu(II) species, without the presence of Al atoms. The lack of correlation between the activity in SCR of NO and the oxidation of NO – NO_2 suggests that the two reactions are competitive.

Zeolite $\text{Cu}_{1.8}\text{SiBEA}$ with mixture of lattice mononuclear and extra-lattice polynuclear Cu(II) species is less active in SCR of NO by ethanol than $\text{Cu}_{1.4}\text{SiBEA}$ with much lower selectivity toward N_2 (85–52%) and much higher selectivity toward NO_2 (maximum 50% at 775 K) due to full oxidation of NO on extra-lattice octahedral Cu(II) species.

Further investigations are undertaken by in situ EPR and FTIR spectroscopy of adsorbed CO and NO to better describe the Cu sites present in Cu_xSiBEA zeolites and active in SCR of NO .

Acknowledgment S.D. gratefully acknowledges the CNRS (France) for financial support as Assistant Researcher.

References

1. Iwamoto M, Furukawa H, Mine Y, Uemura F, Mikuriya S, Kagawa S (1986) *J Chem Soc Chem Commun* 1272
2. Iwamoto M, Mizuno N, Yahiro H (1993) *Stud Surf Sci Catal* 75:1285
3. Iwamoto M, Yahiro H, Tanda K, Mizuno N, Mine Y, Kagawa S (1991) *J Phys Chem* 95:3727
4. Li Y, Hall WK (1991) *J Catal* 129:202
5. Moden B, Da Costa P, Lee DK, Iglesia E (2002) *J Phys Chem B* 106:9633
6. Moretti G (1994) *Catal Lett* 28:143
7. Dzwigaj S, Peltre MJ, Massiani P, Davidson A, Che M, Sen T, Sivasanker S (1998) *J Chem Soc Chem Commun* 87
8. Dzwigaj S, Massiani P, Davidson A, Che M (2000) *J Mol Catal* 155:169
9. Cambor MA, Corma A, Pérez-Pariente J (1993) *Zeolites* 13:82
10. Reddy JS, Sayari A (1995) *Stud Surf Sci Catal* 64:309
11. Jentys A, Pham NH, Vinek H (1996) *J Chem Soc Faraday Trans* 92:3287
12. Moretti G, Dossi C, Fusi A, Recchia S, Psaro R (1999) *Appl Catal B* 20:67
13. Groothaert MH, Van Bokhoven JA, Battiston AA, Weckhuysen BM, Schoonheydt RA (2003) *J Am Chem Soc* 125:7629
14. Groothaert MH, Smeets PJ, Sels BF, Jacobs PA, Schoonheydt RA (2005) *J Am Chem Soc* 127:1394
15. Praliaud H, Mikhailenko S, Chajar Z, Primet M (1998) *Appl Catal B* 16:359
16. Shimizu KI, Maruyama R, Hatamachi T, Kodama T (2007) *J Phys Chem C* 111:6440
17. Solomon EI, Chen P, Metz M, Lee S, Palmer AE (2001) *Angew Chem Int Ed* 40:4571
18. Grünert W, Hayes NW, Joyner RW, Shpiro ES, Siddiqui MRH, Baeva GN (1994) *J Phys Chem* 98:10832
19. Corma A, Palomares A, Márquez F (1997) *J Catal* 170:132
20. De Lucas A, Valverde JL, Dorado F, Romero A, Asencio I (2005) *J Mol Catal A* 225:47
21. Matsumoto H, Tanabe S (1999) *J Chem Soc Chem Commun* 875
22. Dossi C, Fusi A, Recchia S, Psaro R, Moretti G (1999) *Micro-porous Mesoporous Mater* 30:165
23. Zhang Y, Drake IJ, Bell AT (2006) *Chem Mater* 18:2347
24. Moreno-Tost R, Santamaria-Gonzalez J, Rodríguez-Castellon E, Jimenez-Lopez A, Autie MA, Gonzalez E, Glacial MC, de las Pozas C (2004) *Appl Catal B* 50:279
25. Chen XY, Shen SC, Chen HH, Kawi S (2004) *J Catal* 221:137
26. Janas J, Machej T, Gurgul J, Socha RP, Che M, Dzwigaj S (2007) *Appl Catal B* 75:239
27. Dzwigaj S, Janas J, Machej T, Che M (2007) *Catal Today* 119:133